

Supporting Information

Concurrently enhanced dielectric property and energy density in poly(vinylidene fluoride)-based core-shell BaTiO₃ nanocomposites via constructing polar and rigid polymer interfacial layer

Cuilian Ding,^a Xinxuan Tang,^a Shiqi Yu,^a Sheng Chen,^{*a} Zijin Liu,^{*b} Hang Luo^c and
Dou Zhang^c

- a. *Key Laboratory of Polymeric Materials and Application Technology of Hunan Province, College of Chemistry, Xiangtan University, Xiangtan 411105, Hunan Province, China. E-mail: chensheng0729@xtu.edu.cn*
- b. *School of Textile Materials and Engineering, Wuyi University, Jiangmen, Guangdong 529020, China. E-mail: jianchijin@126.com*
- c. *State Key Laboratory of Powder Metallurgy, Central South University, Changsha, Hunan 410083, China*

1. Characterization

Nuclear magnetic resonance (NMR) measurements of the monomers and corresponding polymers were carried out on a Bruker ARX400 MHz spectrometer using CDCl₃ and d₆-DMSO as solvents, tetramethyl silane (TMS) as the internal standard at room temperature. Fourier-transform infrared (FT-IR) spectroscopy was performed with a Nicolet 6700 instrument over the range of 4000~600 cm⁻¹ to identify the functionalization of the samples. Thermogravimetric analysis (TGA) of the samples was executed on a TA SDT Q600 instrument at a heating rate of 10°C/min in a nitrogen atmosphere. The morphology of raw BaTiO₃ nanoparticles, modified BaTiO₃ nanoparticles and nanocomposites were characterized by scanning electron microscopy (SEM, JSM-6390) and by transmission electron microscopy (TEM, JEOL JEM-2100). Differential scanning calorimetry (DSC) heating and cooling curves of neat PVDF and the nanocomposites were obtained using on a TA Q25 DSC instrument under a nitrogen atmosphere. The samples were firstly heated from room temperature to 200 °C at the rate of 10 °C/min in order to eliminate the thermal history, then cooled to -50 °C at the

same rate. Next, the sample was heated from $-50\text{ }^{\circ}\text{C}$ to $200\text{ }^{\circ}\text{C}$ at the rate of $5\text{ }^{\circ}\text{C}/\text{min}$, and finally cooled to $40\text{ }^{\circ}\text{C}$ at the rate of $5\text{ }^{\circ}\text{C}/\text{min}$. The liquid crystalline texture of the polymers was observed under polarized optical microscopy (POM, Leica DM-LMP) equipped with a Mettler-Toledo hot stage (FP82HT). 1D WAXD experiments were performed on a BRUKER AXS D8 advance diffractometer with a 40 kV FL tubes as the X-ray source (Cu Ka) and a LYNXEYE_XE detector. The prepared samples were tested at a scanning rate of $1^{\circ}/\text{min}$ over the range of $10^{\circ} \leq 2\theta \leq 60^{\circ}$. The frequency-dependent dielectric constant, dielectric loss and conductivity of the polymers were measured using an Agilent 4294A LCR meter with a frequency range from 10^3 Hz to 10^7 Hz and 1 V applied voltage. The polarization-electric field hysteresis loops of the composites were performed at 200 Hz by a TF analyzer 2000 ferroelectric polarization tester (aixACT, Germany). The energy storage performance was calculated on the basis of the P-E loops. The pulse discharge performance was tested by dielectric material charge measurement system (DCQ-20A, PolyK Technologies, USA)

2. Synthesis of the Monomers

In the first step, 2-vinylterephthalic acid (4.1 g, 21 mmol), the right amount of SOCl_2 , a suitable size PTFE magnetic agitator, two drops of nitrobenzene solution and two drops of refined DMF were successively added into a dry and spotless 50 mL round-bottom flask. Afterwards, the round-bottom flask was placed in a $60\text{ }^{\circ}\text{C}$ oil bath and the hybrid solution was refluxed until the mixed solution turned into transparent. After continuing to react for an hour, the flask was left standing and cooled. Then, the blended solution was rotated with a rotary evaporator to dislodge redundant SOCl_2 , and the residue was washed with dried petroleum ether several times. The yellow oily substance was finally obtained by disposing of the petroleum ether via a rotary evaporator.

In the second step, 4-cyanophenyl (5.6 g, 47 mmol), DMAP (5.2 g, 43 mmol), purified Et_3N (10.8 g, 107 mmol) and an appropriate amount of dried CH_2Cl_2 solution were successively added into a 250 mL round-bottom flask, which labeled as system A. In the meantime, the yellow oily substance was dissolved in dried CH_2Cl_2 solution and added into a 100 mL constant pressure drop funnel, which denoted as system B. After that, under continuous stirring, system B was dropped into system A at a rate of

1/3 drop/s. It should be noted that this reaction process should be carried out in an ice bath. After 12 h, the reaction was stopped and the excess solvent was removed by a rotary evaporator. The resulting mixture was dissolved in a handful of CH_2Cl_2 , and extracted several times in turn with the appropriate concentration of saturated NaHCO_3 solution and deionized water. The collected organic phase was dried with anhydrous MgSO_4 , and then the destination product was purified in a silica gel column (the eluent is a mixture of CH_2Cl_2 and petroleum ether). Eventually, the prepared sample was dissolved in a small amount of CH_2Cl_2 solvent, and slowly added into a beaker containing a large amount of petroleum ether. Meanwhile, the precipitates appeared in the solution. After centrifugation, the precipitates were collected and dried under vacuum for 24 h. The target monomer vinyl terephthalate bis (4-cyanophenyl) ester (m-BCN) was procured. Taking the similar procedure, the monomer vinyl terephthalate bis (4-cyanoethyl) ester (m-ECN) was obtained.

3. Preparation of Polymers

First of all, monomer and AIBN at a feeding ratio of 100:1, the right size PTFE magnetic agitator and a proper amount of purified DMF were added into a polymerization tube. Whereafter, the tube underwent liquid nitrogen freezing-vacuuming-nitrogen circulation three times to guarantee that the air in the glass tube was dislodged. After that, the tube was vacuum sealed with an alcohol blowtorch and then was quickly transferred to a 75 °C preheated oil bath. After 24 h, the tube was removed and immersed in ice water to cool, and then the top of the tube was broken with tweezers. Lastly, polymer solution was diluted with a little DMF solvent, and immediately added into a conical flask containing a large amount of iced methanol to precipitate. The destination polymer (PBCN and PECN) was obtained by centrifugation and vacuum drying.

4. Surface modification of BaTiO_3 nanoparticles

(1) Hydroxylation of BaTiO_3 nanoparticles was implemented (BT-OH). First, 11 g initial BT nanoparticles were dispersed into 120 mL H_2O_2 solution, followed by ultrasonic treatment for 30 min. Then, the mixture was refluxed at 106 °C for 6 h. The nanoparticles were regained by centrifugation at 4000 rpm for 10 min, and washed with

deionized water for five times. Ultimately, the nanoparticles (BT-OH) were dried in a vacuum drying oven at 80 °C for 24 h.

(2) The BaTiO₃ nanoparticles were aminated by γ -APS (γ -APS@BT). 10 g BT-OH nanoparticles were dispersed into 100 mL refined THF solution and ultrasound for 30 min. After that, 8 g γ -APS was added and the mixture was refluxed at 80 °C for 24 h under the protection of N₂ atmosphere. The nanoparticles (γ -APS@BT) were obtained by centrifugation at 4000 rpm for 10 min, washed with THF solvent for five times and dried at 80 °C for 24 h.

(3) The formerly activated RAFT agent (CPDB-NHS) was connected to the surface of BaTiO₃ nanoparticles (CPDB@BT).¹ 5 g γ -APS@BT nanoparticles were dispersed in 100 mL THF solution and ultrasound for 30 min. Next, it was slowly dropped into the THF solution of CPDB-NHS under ice bath conditions, and the mixture was stirred at 20 °C for 12 h. After centrifugation, washing with THF solvent and removing solvent at 60 °C, the product (CPDB@BT) was collected.

(4) Vinyl terephthalate bis (4-cyanophenyl) ester (m-BCN) and vinyl terephthalate bis (3-hydroxypropyl) ester (m-ECN) were grafted onto the surface of BT nanoparticles through RAFT polymerization, respectively. Taking monomer m-BCN as an example, the synthetic process was described as follows. CPDB@BT (1 g), monomer m-BCN (1 g), AIBN (4.1 mg) and dehydrated DMF (9.0 g) were added to a polymerization tube. Then, the tube underwent liquid nitrogen freezing-vacuums-nitrogen circulation three times to ensure that the air in the glass tube was removed. The tube was sealed with an alcohol blowtorch and was put into the oil bath at 75 °C. After stirring continuously for 24 h, the tube was immersed into ice water to terminate the polymerization reaction. Next, the tube was broken and the polymer reaction solution was diluted with bits of THF solution. The final core-shell nanoparticles (PBCN@BT or PECN@BT) were centrifuged at 4000 rpm for 10 min, and washed with THF solvent for five times, and dried at 60 °C for 24 h.

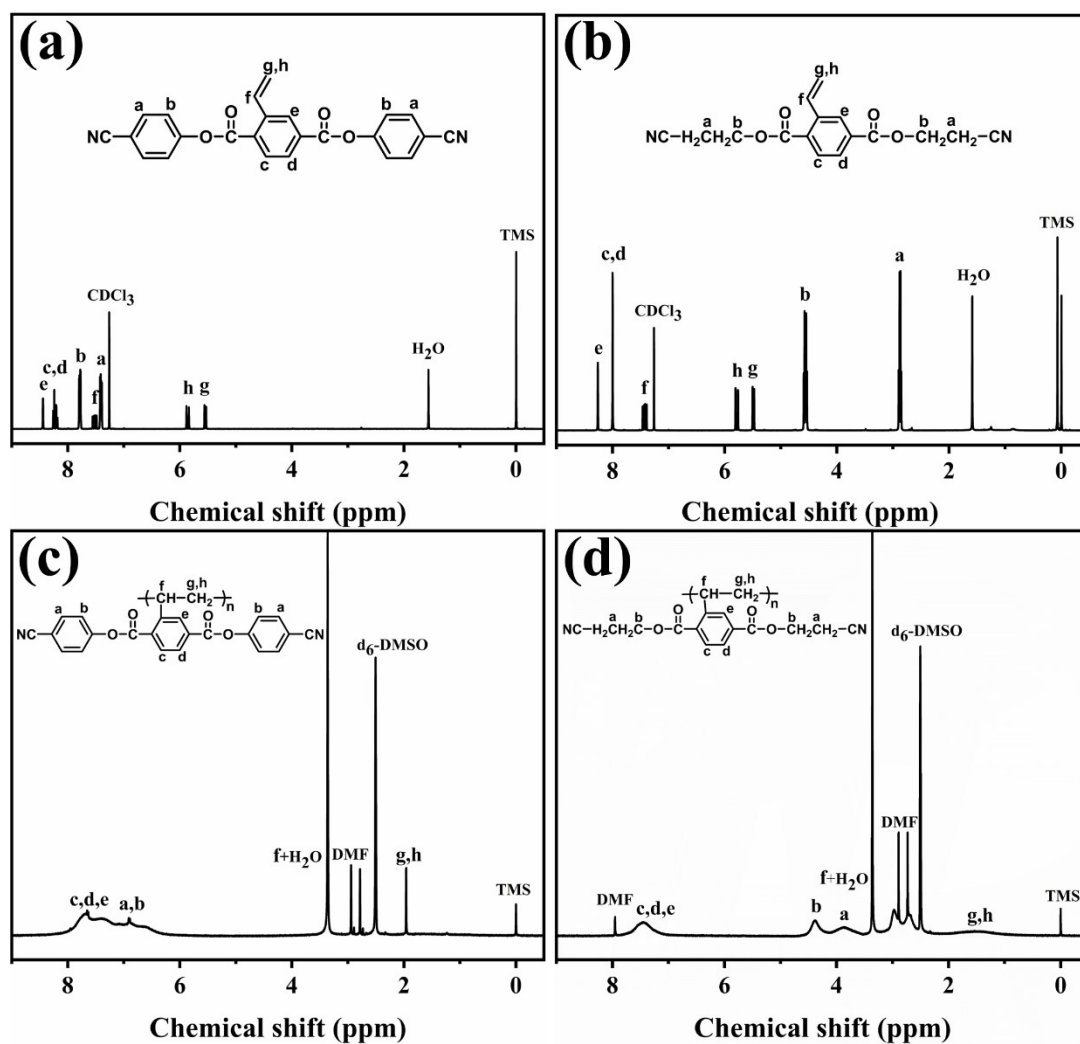


Figure S1. ^1H NMR spectra of the monomers in CDCl_3 and polymers in d_6 -DMSO:

(a) m-BCN, (b) m-ECN, (c) PBCN and (d) PECN.

Table S1. The thickness of the PVDF-based nanocomposited freestanding films

Sample	Thickness (μm)	Sample	Thickness (μm)
PVDF	12	PVDF	12
1 vol%-PBCN@BT/PVDF	14	1 vol%-PECN@BT/PVDF	12
3 vol%-PBCN@BT/PVDF	14	3 vol%-PECN@BT/PVDF	13
5 vol%-PBCN@BT/PVDF	13	5 vol%-PECN@BT/PVDF	13
7 vol%-PBCN@BT/PVDF	12	7 vol%-PECN@BT/PVDF	14
9 vol%-PBCN@BT/PVDF	14	9 vol%-PECN@BT/PVDF	13

Table S2. Absorption data of the cyano-polymers films and calculated band-gap

Sample	λ_{\max} (nm)	$\lambda_{\text{on-set}}$ (nm)	$E_{\text{opt}} \text{ g(eV)}^{\text{a}}$
PBCN	298	360	3.44
PECN	298	328	3.78

^a Calculated optical band-gap using
$$E_g^{\text{opt}} = \frac{1240}{\lambda_{\text{on-set}}}$$

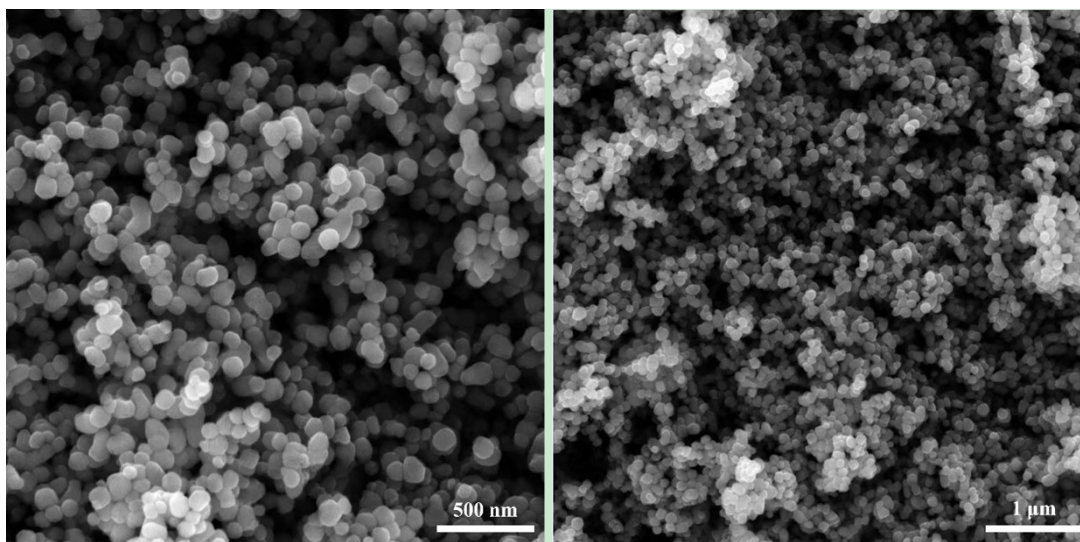


Figure S2. SEM images of the as-received BT nanoparticles.

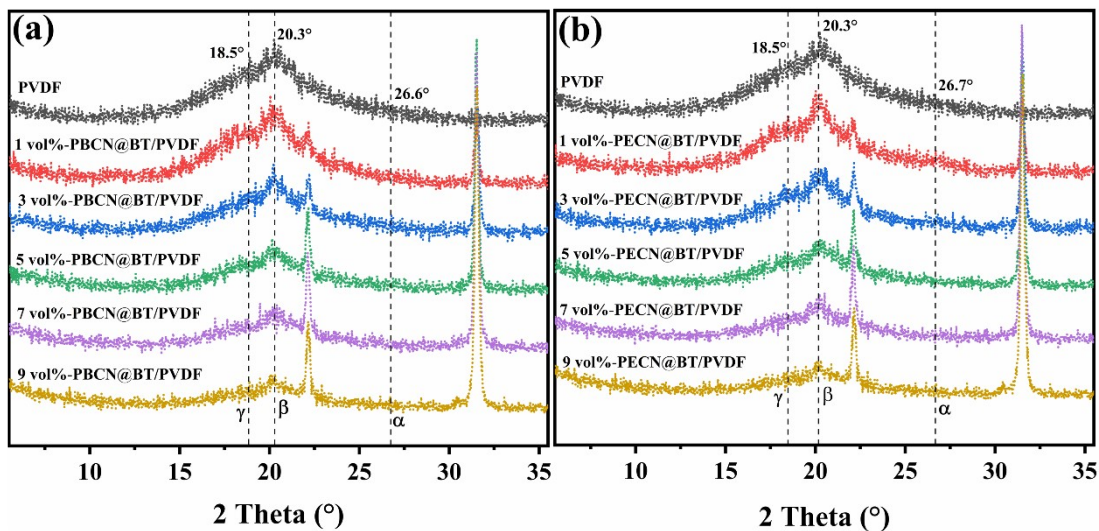


Figure S3. XRD diffraction patterns of (a) PBCN@BT/PVDF nanocomposites and (b) PECN@BT/PVDF nanocomposites.

Table S3. Physical properties of cyano-polymer@BT/PVDF nanocomposites

Sample	T_c (°C) ^a	T_m (°C) ^b	ΔH_m (J/g) ^c	χ_c (%) ^d
PVDF	146.81	171.87	53.99	51.62
1 vol%-PBCN@BT/PVDF	146.90	171.87	52.60	52.14
3 vol%-PBCN@BT/PVDF	147.42	171.89	51.51	54.77
5 vol%-PBCN@BT/PVDF	148.55	171.95	48.69	55.43
7 vol%-PBCN@BT/PVDF	148.47	171.83	44.19	53.84
9 vol%-PBCN@BT/PVDF	149.08	171.86	40.81	52.99
1 vol%-PECN@BT/PVDF	147.57	171.97	54.99	54.52
3 vol%-PECN@BT/PVDF	148.15	171.95	52.85	56.19
5 vol%-PECN@BT/PVDF	148.09	171.77	52.42	59.68
7 vol%-PECN@BT/PVDF	148.76	171.81	47.62	58.02
9 vol%-PECN@BT/PVDF	148.58	171.93	44.10	57.26

^a Crystallization temperature (T_c) was measured by DSC at a cooling rate of 5°C/min under N₂ during the first cooling process.

^b The melting temperature (T_m) was measured by DSC at a heating rate of 5°C/min under N₂ during the second heating process.

^c Melting enthalpy (ΔH_m).

^d Crystallinity (χ_c).

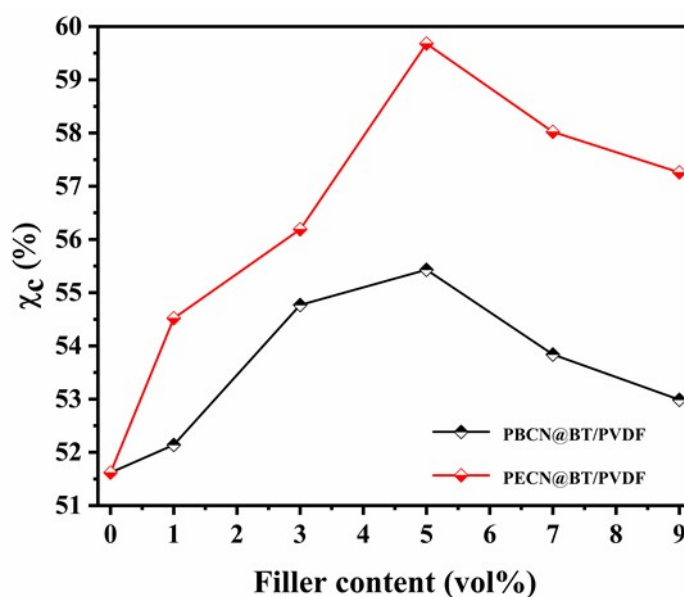


Figure S4. Crystallinity of neat PVDF film and PVDF-based nanocomposites with

different filler content of modified nanoparticles.

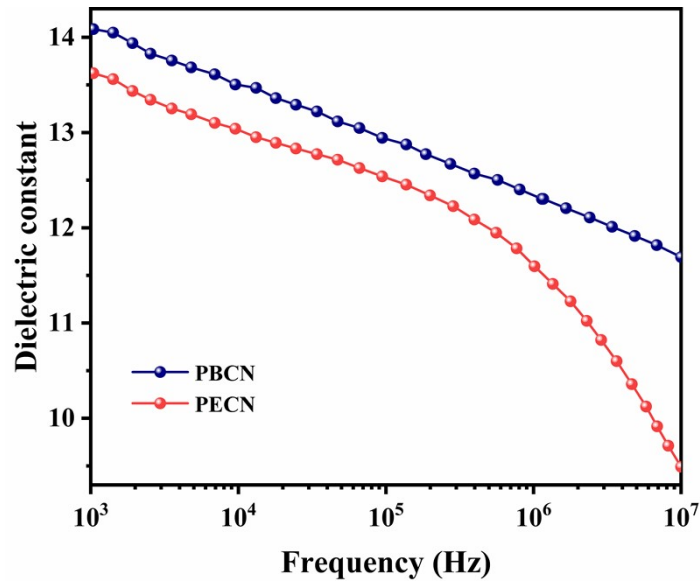


Figure S5. Frequency dependence of dielectric constant of PBCN and PECN.

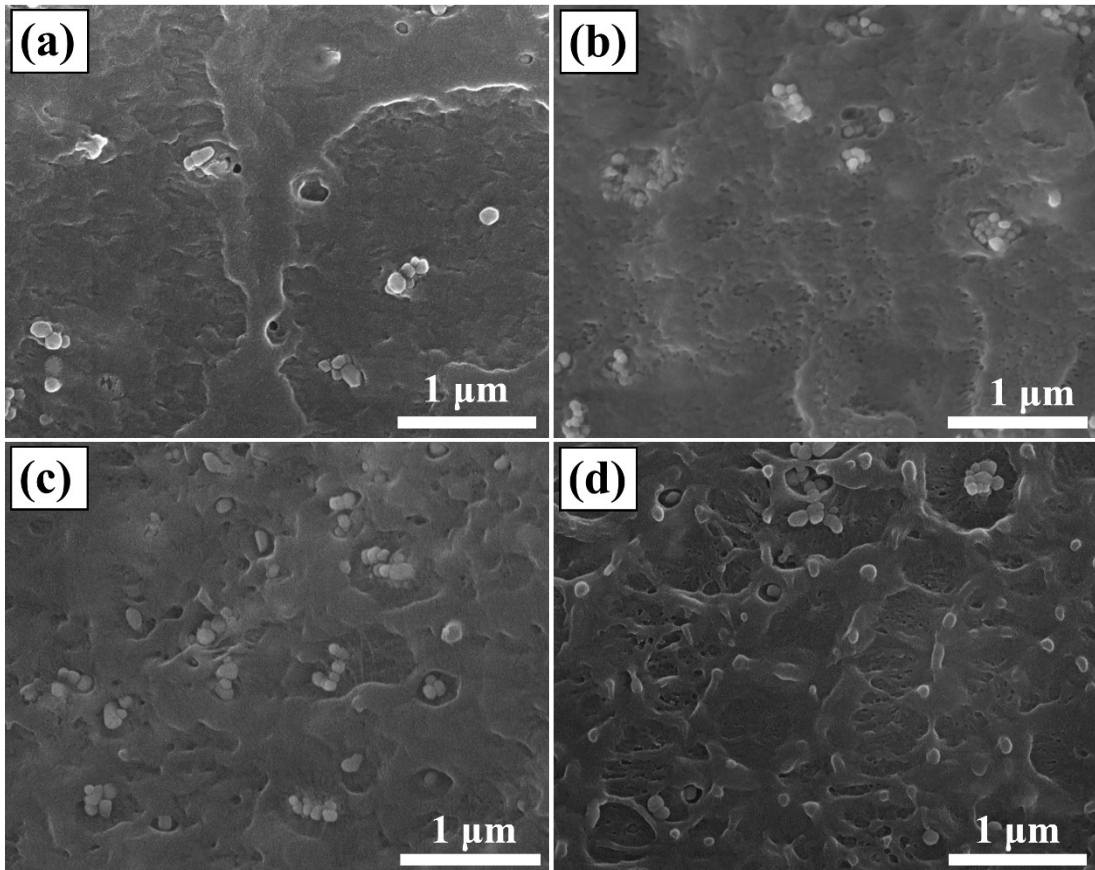


Figure S6. SEM images of the freeze-fractured cross-sectional morphologies of the nanocomposite films: (a) 7 vol%-PBCN@BT/PVDF, (b) 7 vol%-PECN@BT/PVDF, (c) 9 vol%-PBCN@PVDF and (d) 9 vol%-PECN@BT/PVDF.

NOTES AND REFERENCES

1. C. Li, J. Han, C. Y. Ryu, and B. C. Benicewicz, *Macromolecules*, 2006, **39**, 3175-3183. .